RSC Advances

REVIEW

View Article Online
View Journal | View Issue

Cite this: *RSC Adv.*, 2022, **12**, 4852

Selective strategies for antibacterial regulation of nanomaterials

Jinliang Ma, *[ab] Kexin Li[a] and Shaobin Gu *[a]

Recalcitrant bacterial infection, as a worldwide challenge, causes large problems for human health and is attracting great attention. The excessive antibiotic-dependent treatment of infections is prone to induce antibiotic resistance. A variety of unique nanomaterials provide an excellent toolkit for killing bacteria and preventing drug resistance. It is of great importance to summarize the design rules of nanomaterials for inhibiting the growth of pathogenic bacteria. We completed a review involving the strategies for regulating antibacterial nanomaterials. First, we discuss the antibacterial manipulation of nanomaterials, including the interaction between the nanomaterial and the bacteria, the damage of the bacterial structure, and the inactivation of biomolecules. Next, we identify six main factors for controlling the antibacterial activity of nanomaterials, including their element composition, size dimensions, surface charge, surface topography, shape selection and modification density. Every factor possesses a preferable standard for maximizing antibacterial activity, providing universal rules for antibacterial regulation of nanomaterials. We hope this comprehensive review will help researchers to precisely design and synthesize nanomaterials, developing intelligent antibacterial agents to address bacterial infections.

Received 12th December 2021
Accepted 25th January 2022

DOI: 10.1039/d1ra08996j

rsc.li/rsc-advances

1. Introduction

Infectious diseases arising from pathogenic bacteria pose serious threats to public health, leading to increased morbidity and mortality.[1,2] A variety of antibiotics have been widely utilized to control the growth of bacteria by inhibiting cell wall synthesis and the functions of essential proteins, DNA and RNA since the first discovery of penicillin in 1928.[3,4] However, with excessive use of the available antibiotics, the treated bacteria have started to adapt to adverse living conditions through gene mutation and transfer, resulting in antibiotic resistance, which is a worldwide challenge.[5,6] This escalating challenge has contributed to an urgent need to develop new antibacterial agents to alleviate the "superbugs" emerging from antibiotic resistance. In addition to designing and synthesizing new antibiotics to address the increasing challenge,[7] researchers are devoting more efforts to look for more alternative strategies in a variety of fields,[8,9] such as the improved antibiotic sensitization of bacteria based on biological regulation,[10,11] the innovative development of antimicrobial peptides and protein toxins,[12,13] and the personalized design of antibacterial nanomaterials.[14,15]

Especially, due to their unique physiochemical properties, antibacterial nanomaterials have provided a robust toolkit for combating drug-resistant pathogenic bacteria and avoiding the emergence of antibiotic resistance, these materials include metal-based substances,[16–19] polymeric nanostructures,[20–22] and carbon-based nanomaterials.[23] Their antibacterial activity arises from damage of the bacterial membrane and inactivation of biomolecules to impede the normal cellular function of the bacteria.[24] For example, in metal nanoparticles (NPs), most of the studied silver NPs (AgNPs) possess excellent antibacterial activity against a series of pathogenic bacteria, contributing to their potential application in medical devices and consumer products.[25,26] Their antimicrobial activity is exerted due to the silver cations released from the AgNPs.[15,27,28] During the antibacterial reaction, the contact surface area and charge on the NPs are two main factors for regulating the binding of the NPs with the cell membrane, destroying the membrane integrity.[29–31] In addition, AgNP-induced formation of reactive oxygen species (ROS) leads to the death of the bacteria.[32] The stability of metal NPs is important to realize their antibacterial properties, where a too unstable or too stable structure may not be preferable.[33–35] Polymeric nanostructures obtained *via* self-assembly, such as phosphonium-functionalized polymer micelles and povidone-iodine-based polymeric nanoparticles, have high antibacterial activity.[36,37] Their antibacterial activity is relative to the controllability of their length and the charge of the polymer. Carbon-based nanomaterials (CNMs) with lower toxicity and higher safety can be endowed with antibacterial activities[23] by

[a]*College of Food and Bioengineering, Henan University of Science and Technology, Luoyang, Henan 471023, China. E-mail: majin1987610@126.com; shaobingu@haust.edu.cn*

[b]*Institute of Molecular Medicine, Renji Hospital, School of Medicine, Shanghai Jiao Tong University, Shanghai 200127, China*

regulating their lateral sizes, shapes, layer numbers, and surface charges.[38–40] Therefore, many strategies can regulate the antibacterial activity of nanomaterials. The reported relevant reviews have focused on the mechanisms and molecular targets of the antimicrobial activity of metals,[14] the biological action of antibacterial silver with different forms,[16,27,41] the antibacterial efficiency of gold nanoparticles (AuNPs) with nonantibiotic or antibiotic molecules,[42] the antibacterial properties and surface functionality of different NPs,[15,43–46] and the role of designed nanomaterials in eradicating bacteria in biofilms.[47] However, the universal relationship between the antibacterial activity and properties of different nanomaterials has not been understood systematically. The confirmation of clear design rules is very important to build customized antibacterial nanomaterials.

In this review, we categorize the antibacterial mechanisms of different nanomaterials and the key factors for controlling their antibacterial activity, providing selective strategies for regulating antibacterial nanomaterials (Fig. 1). To begin with, we discuss how the nanomaterials interact with the bacteria and destroy the bacterial structure to exert their antibacterial activity. Next, we mainly review six factors for regulating the antibacterial activity of nanomaterials, including their element composition, size dimension, charge type, surface topography, shape selection, and modification density. In addition, two other factors, namely stiffness and hydrophobicity, are listed briefly. We hope that this comprehensive review can help researchers precisely customize nanomaterials to meet the requirements for developing intelligent antibacterial agents.

2. Antibacterial manipulation of nanomaterials

Based on their unique physiochemical properties, nanomaterials exert antibacterial activity according to three main bactericidal pathways (Fig. 2). The integrity of the cell membrane is destroyed with initial binding of the nanomaterials to the bacterial surface, causing possible leakage of intracellular molecules (1).[48] The composition, charge type, surface topography, and modification density of the nanomaterials are of great significance to regulate the initial interaction of the nanomaterials and bacteria. After penetrating into the bacterial cell membrane, nanomaterials interact with various biomolecules in the cell, such as DNA, ribosomes and enzymes, disturbing the function of biomolecules, such as DNA replication, protein synthesis, and molecular catalysis (2).[49,50] The size and shape of nanomaterials can affect their entry into bacterial cells. The inherent properties of nanomaterials with different compositions disturb the activity of biomolecules in the cells. In addition, with the addition of nanomaterials with different compositions and charges, oxidative stress and electrolyte imbalance are induced in the cell, causing death of the bacterial cell due to a lack of normal cellular behaviour (3).[24] Therefore, the operation of bactericidal pathways depends on the core structure, size, shape, and surface status of the nanomaterials, which is of great significance to regulate their interaction with bacteria and biomolecules, obtaining broad-spectrum antibacterial activity and simultaneously reducing their toxicity against mammalian cells.

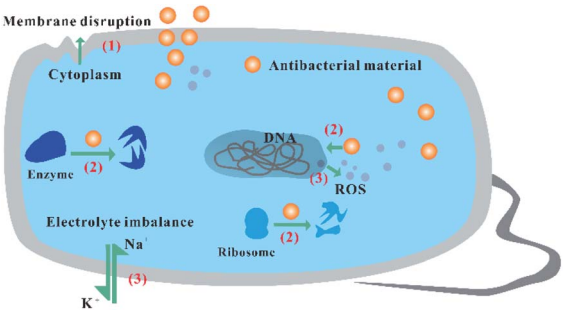

Fig. 2 The fundamental antibacterial performance of nanomaterials according to different bactericidal pathways.

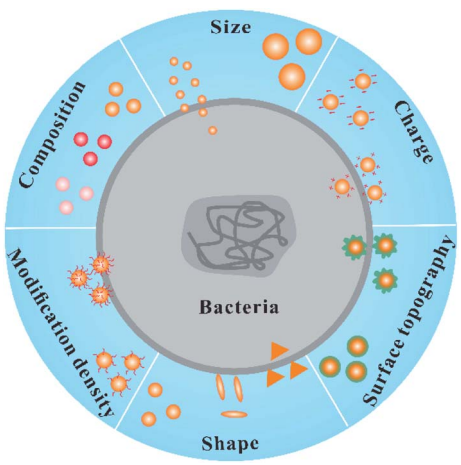

Fig. 1 The main factors for regulating the antibacterial activity of nanomaterials: composition, size, charge, topography, shape and modification density.

3. Selective strategies for the antibacterial regulation of nanomaterials

3.1. Composition

Nanomaterials with different inherent compositions perform different antibacterial reactions. Metal-based NPs with different sizes in the range of 1–100 nm, such as silver, copper, gold, zinc and titanium, produce different physicochemical, electrical, optical, and biological properties. AgNPs release free Ag^+ ions as active agents, destroying the bacterial membrane and disrupting electron transport and DNA function.[51] The bactericidal effect appears in copper NPs (CuNPs) due to the formation of ROS *via* the function of copper-containing nanozymes.[45,46] In addition to ROS-induced bactericidal effects, CuNPs can degrade into copper ions to enter the bacterial cell, destroying functions of DNA and RNA.[52,53] Degradable Cu-doped phosphate-based glass (Cu-PBG) can simultaneously generate ROS and release copper ions, leading

to excellent antibacterial effects (Fig. 3).[54] Different from silver and copper, gold does not readily dissociate into ions due to its higher inertness and stability.[55] It is necessary to endow AuNPs with antibacterial activity by grafting some compounds on their surface. Nanomaterials based on ZnO and TiO_2 also cause cell membrane damage and generate ROS, killing the bacteria.[15,43,56] In addition to metal-based NPs, using different synthesis methods, carbon atoms have been interconnected to form a variety of conventional CNMs, such as carbon dots, graphene quantum dots, carbon nanotubes (CNTs), and graphene oxide (GO). The CNMs can induce physical damage of the bacterial outer membrane or cell wall to exert antibacterial activity. For example, GO as a surface oxygen carrier can perform knife-like or lipid-extraction membrane destruction[57,58] and oxidation reactions, leading to the death or inactivation of bacteria.[59] CNTs can act as "nanodarts" to penetrate across the bacterial cell membrane.[60–62] With the generation of ROS *via* electron transfer from their interaction with bacterial molecules, CNTs can inactivate proteins, lipids and nucleic acids to kill the bacteria.[40]

3.2. Size

The extraordinary properties of the materials are tailored *via* precise control on the molecular and atomic scales.[63,64] The size-dependent characteristics of the nanomaterials contribute to their particular applications in surface-enhanced Raman scattering (SERS), green catalysts, and superior magnetic resonance imaging.[65–68] More importantly, the regulation of size endows the nanomaterials with tunable physiological properties, including cell uptake, biodistribution, pharmacokinetics, cytotoxicity, and targeting efficiency.[69–74] Especially focusing on the specific cytotoxicity of nanomaterials to bacteria, by decreasing the size of the materials from NPs to nanoclusters (NCs), the antimicrobial activity of broad-spectrum nanomaterials has been enhanced, effectively avoiding antimicrobial resistance.[75,76] For example, ultrasmall gold NCs (AuNCs) readily interact with bacteria (*Staphylococcus aureus* as model bacteria), producing high antimicrobial activity with a wide spectrum. In the process, metabolic imbalance occurs after the internalization of AuNCs into bacterial cells. Subsequently, the increased ROS in the bacterial cell causes the death of bacteria (Fig. 4A).[77] The inert and inactive AuNPs can be endowed with antibacterial activity by decreasing the size of the NPs.

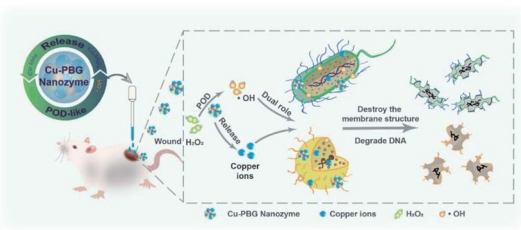

Fig. 3 Cu-PBG-mediated antibacterial activity due to the formation of ROS and the release of copper ions.[54] Reproduced from ref. 54 with permission from the American Chemical Society, Copyright© 2021.

In addition to gold-based nanomaterials, the size of zinc oxide NPs (ZnO NPs) plays a significant role in the antibacterial activity of NPs, where smaller ZnO NPs have higher antibacterial efficiency.[78,79] Similarly, the antibacterial activity of ZnO NPs is attributed to both ROS generation and NP accumulation in the bacteria. Due to their enhanced contact surface area, compared with larger NPs, smaller AgNPs ranging from 1 to 10 nm more readily bind to the surface of the cell membrane, disturbing the permeability and respiration of the cell.[31,80] The increased reactive groups make the NPs produce higher toxicity.[81–83] The AgNPs, after entry into the bacterial cell, interact with the thiol groups of proteins, preventing the synthesis of ribosomal subunits, the activity of cellular components,[80] and the function of DNA replication.[84,85]

The precise size control of the nanomaterials depends on the ligand modification on the structural surface. The number and species of the ligands endow the nanomaterials with the defined size and stability. Cationic AuNPs with sizes of 6 nm (NP1) and 2 nm (NP2) displayed different cell lysis behaviours against bacteria.[87] NP1 and NP2 were synthesized *via* place exchange of undecanethiol-capped AuNPs[88] and pentanethiol-capped AuNPs, respectively.[89] NP2 (2 nm) are more toxic than NP1 (6 nm) against *Bacillus subtilis*.[87] Using one of two different zwitterionic ligands (SN or NS ligand), the effective antibacterial activity of AuNPs can be obtained through modulation of the NP size (2, 4, and 6 nm). Different from the higher antibacterial activity with smaller size, AuNPs stabilized by zwitterionic ligands (oligo(ethylene glycol)-functionalized interior) showed increased antimicrobial efficiency with increased size through bacterial membrane disruption (Fig. 4B and C).[86] As the size changed from 2 to 6 nm, the MIC concentration of zwitterionic AuNPs against *Pseudomonas aeruginosa* could decrease from 8000 to 50 nM. Compared with smaller NPs (2 nm) with disorganized shells of ligands, larger NPs (>4.4 nm) with ordered "2D-like" surfaces more readily interact with the cell surface. In the design of nanomaterials, we should fully consider the action of the ligands when seeking a small size for improving the antibacterial activity.

Although the resistance of bacteria to nanomaterials has a lower occurrence than their resistance to antibiotics, it remains present.[47,90] Size regulation can prevent drug resistance. 4,6-Diamino-2-pyrimidine thiol (DAPT)-capped AuNPs (DAPT-AuNPs) with a positive charge readily absorb on the negatively charged surfaces of bacteria.[51,91,92] After *Escherichia coli* was cultured 183 successive times using DAPT-AuNPs with increased concentrations, DAPT-AuNP-resistant *E. coli* were obtained. The bactericidal activities of DAPT-AuNPs to the resistant strain were recovered by tuning the size of the DAPT-AuNPs without introduction of new chemicals (Fig. 5).[18] Size regulation can act as an alternative strategy for avoiding drug resistance of nanomaterials.

The size-dependent antibacterial activity of some nanomaterials is shown in Table 1. The MIC of nanomaterials with sizes of 1.8–12 nm changes from 50 nM to 7 mM, or several μg mL^{-1}. However, an accurate antibacterial comparison between different size-dependent nanomaterials is difficult to perform

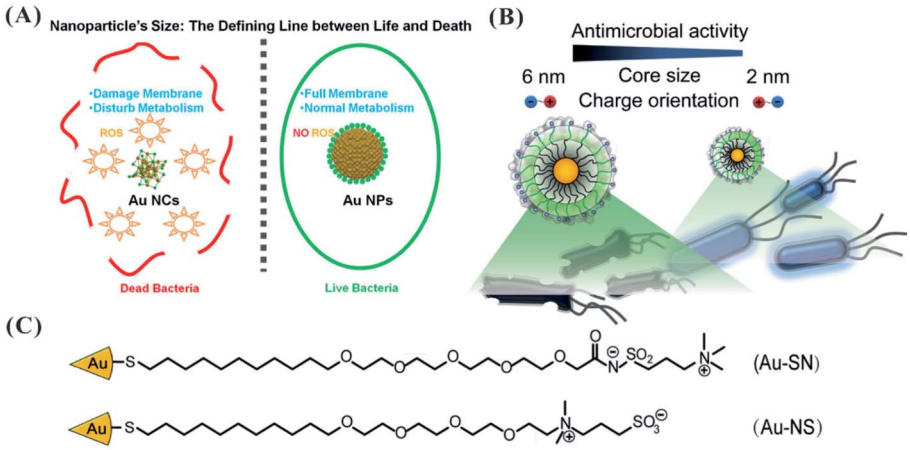

Fig. 4 (A) The enhanced antibacterial activity of AuNCs relative to AuNPs due to the formation of ROS.[77] Reproduced from ref. 77 with permission from the American Chemical Society, Copyright© 2017. (B) Controllability of the antibacterial activity of AuNPs by regulating the NP size.[86] (C) The ligand structure for the synthesis of AuNPs.[86] Reproduced from ref. 86 with permission from the American Chemical Society, Copyright© 2016.

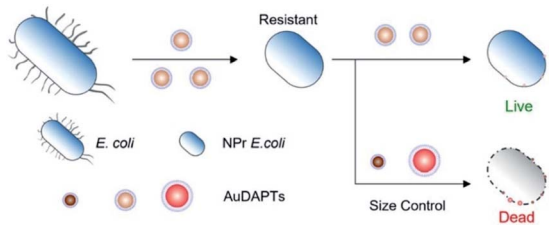

Fig. 5 Schematic design of size-specific resistance of *E. coli* to DAPT-AuNPs.[18] Reproduced from ref. 18 with permission from the American Chemical Society, Copyright© 2021.

due to the disturbance of different selected ligands and indicator bacteria.

3.3. Charge

The adhesion events of nanomaterials and bacteria depend on force interactions (including static electricity, hydrophobicity and van der Waals) and receptor–ligand recognition.[24] Ligands with positively charged, negatively charged, and/or zwitterionic moieties have been immobilized onto the surface of NPs, providing the basis for the adhesion action of nanomaterials and bacteria. Teichoic acids and lipopolysaccharide are characteristic components in the cell walls of Gram-positive and Gram-negative bacteria, respectively. Phosphate groups (also carboxylates in Gram-negative bacteria) in the structure endow bacterial surfaces with a negative charge.[44] Usually, ligands with cationic groups are considered to be ideal candidates for designing and regulating antibacterial agents.[93] Multiple cationic antimicrobials have been constructed by sufficiently utilizing the facile electrostatic attraction of a cationic agent and negative bacterial surface, such as peptides,[94,95] polymers[96] and NPs.[42,87,97–99] By separately using the ligands 3-mercaptopropionic acid (MPA), 3-mercaptopropylamine ($MPNH_2$), and poly(allylamine hydrochloride) (PAH), three types of AuNPs with different charge compositions were designed. Compared with anionic MPA-AuNPs, cationic PAH-AuNPs with more positive charge provided higher toxicity to bacteria (Fig. 6).[99] Similarly, compared with anionic polymaleic anhydride-*alt*-1-octadecene (PMAO), quantum dots (QDs) coated with cationic polyethylenimine (PEI) exhibited higher inhibition against *Pseudomonas stutzeri*.[100] The growth inhibition and death of the bacteria occurred after introducing these cationic agents according to the following steps. After binding initially with the cell wall, the antibacterial agents further penetrate and interact with lipids or proteins in the cell membrane, leading to membrane disorganization and leakage of small molecules in

Table 1 The size-dependent antibacterial activity of different nanomaterials

No.	Nanomaterial	Ligand	Size (nm)	Bacteria	MIC	Reference
1	AuNCs	6-Mercaptohexanoic acid	<2 nm	*S. aureus*	2.5 μM	77
2	ZnO NPs	Tetramethylammonium hydroxide	~12 nm	*S. aureus*	4 to 7 mM	79
3	AgNPs	Glycol-thiol	3 nm	*E. coli*	6% survival rates at 2.2 mg L^{-1}	28
4	AgNPs	Gallic acid	7 nm	*E. coli*	6.25 μg mL^{-1}	82
5	AuNPs	Hexyl-substituted, ammonium-functionalized thiol	2 nm	*B. subtilis*	80% cell damage at 300 nM	87
6	AuNPs	Zwitterionic ligand	6 nm	*P. aeruginosa*	50 nM	86
7	AuNPs	4,6-Diamino-2-pyrimidine thiol	1.8 nm	*E. coli*	3 μg mL^{-1}	18

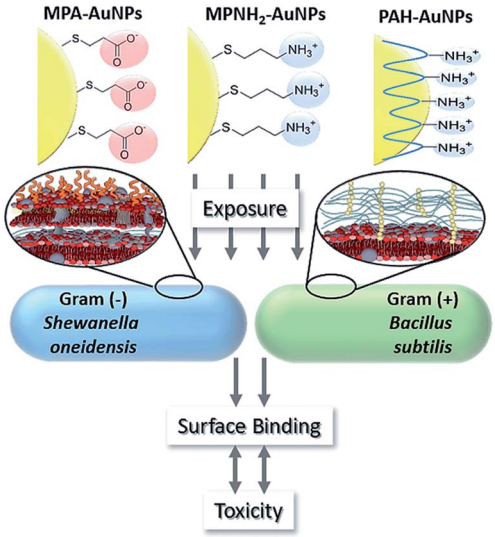

Fig. 6 Antibacterial performance of AuNPs functionalized with anionic or cationic ligands.[99] Reproduced from ref. 99 with permission.

the cell. Finally, the gradual degradation of active biomolecules (such as proteins and nucleic acids) and lysis of bacteria cause the bacterial death.[93]

Quaternary ammonium (QA) compounds are the most frequently used compounds for producing antiseptics and disinfectants. The resin acids in QA can act as an active hydrophobic component to promote antibacterial activity.[101] QA groups more readily interact with the cell membranes of bacteria, leading to disruption of the membranes to execute the antibacterial properties.[102] Cationic poly(*p*-phenyleneethynylene)s (PPEs) with QA can bind advantageously to the surface of bacteria, indicating effective antibacterial activity against various bacteria.[103–105] Using magnetic NPs functionalized with poly(quaternary ammonium) (PQA), 100% biocidal efficiency was still retained after performing the antibacterial cycle eight times.[106] In addition, some polymeric QA compounds (polyquaternium-1) have good selective antimicrobial activity on bacterial and fungous microorganisms. They lead to high antimicrobial activity by destroying the spheroplasts of bacterial *Serratia marcescens*, but they show low inhibition against fungous *Candida albicans* due to the different microbial structures of bacteria and fungi.[107]

In addition to conventional QA as a cationic source, other ammonium-contained agents have been explored for obtaining good antibacterial activity. Positively charged cetyltrimethylammonium bromide (CTAB) was used to coat gold nanorods (AuNRs). CTAB-AuNRs bound with negatively charged teichoic acid in the cell wall of Gram-positive *B. cereus* and deposited on the bacterial surface due to the electrostatic interaction.[108] Based on dimethyldecylammonium chitosan-*graft*-poly(ethylene glycol)methacrylate (DMDC-Q-*g*-EM) and poly(ethylene glycol)diacrylate, a polycationic hydrogel was built to achieve excellent antimicrobial efficacy. Like an 'anion sponge', the polycationic hydrogel drew anionic phospholipids out of the bacterial cell membrane into the gel pores. The positive charge density and pore size of the polycationic hydrogel determined the killing efficacy of the bacteria.[109] However, positively charged NPs can produce substantial toxicity (*e.g.* hemolytic activity) to mammalian cells, resulting in difficulty of their application for killing pathogenic bacteria in infectious diseases.[110,111] Neutral zwitterionic ligands integrated into cationic NPs can decrease their toxicity to mammalian cells while maintaining their antibacterial properties.[112,113] The exquisite balance of zwitterionic and cationic ligands guarantees the stability as well as the antibacterial activity of the NPs.[99,114,115] Using zwitterionic ligands with different charge orientations, several AuNPs were designed. The cationic charge in the outer layer is preferable to the charge inside the layer to perform antimicrobial activity (Fig. 4C).[86]

Although a cationic group is preferable, the origin of the antibacterial activity of nanomaterials is not confined to the modification of positive charge. Negatively charged carboxyl-modified single-walled carbon nanotubes can cause growth inhibition of *Paracoccus denitrificans* due to the influence of bacterial gene expression.[116] In addition to the cationic ligands responsible for the combination of nanomaterials and the bacterial surface, anionic ligands with carboxylate headgroups may disrupt hydrogen bonding within the cell wall during their interaction, leading to cell lysis.[117,118] Due to the different compositions of the cell wall in the two kinds of bacteria, tunable selectivity for two bacterial types was achieved by tailoring the surface chemistry of NPs. NPs functionalized with different ratios of charge indicated different antibacterial activities against Gram-positive and Gram-negative bacteria. The balance between polyvalent electrostatic and non-covalent interactions acts together to disrupt the bacterial cell. Using different ratios of positively charged *N*,*N*,*N*-trimethyl(11-mercaptoundecyl)ammonium chloride (TMA) and negatively charged 11-mercaptoundecanoic acid (MUA) ligands, NPs with different charge ratios were fabricated (Fig. 7A). Different charge ratios induced by the two ligands endowed the NPs with different surface charges (Fig. 7B). NPs with 48 : 52 and 80 : 20 TMA : MUA could selectively kill Gram-positive and Gram-negative bacteria, respectively, at commensurate rates.[119] However, the results did not clarify at the molecular level how NPs with mixed charge selectively interact with the cell wall in Gram-specific bacteria.

In addition to the introduction of negative charge, drugs have been added to coat nanomaterials to enhance their antibacterial activity. AuNPs stabilized by DAPT (DAPT-AuNPs) only sufficiently inhibit Gram-negative bacteria. Synergistic effects were obtained when modifying non-antibiotic amines (NAA) and DAPT (D, pyrimidinethiol) as co-ligands on the surface of AuNPs *via* Au–N and Au–S interactions, forming Au_D/NAA NPs (Fig. 7C).[120] The synergistic effects from the co-ligands of NAA and DAPT are attributed to the increased permeability of both the bacterial cell wall and membranes. The hydroxyl and amido groups from ampicillin were chelated with AgNPs to form an AgNP–ampicillin complex. The ampicillin-induced damage of the bacterial cell wall enhanced the penetration of AgNPs into the cell to bind with DNA, producing better antimicrobial effects.[121]

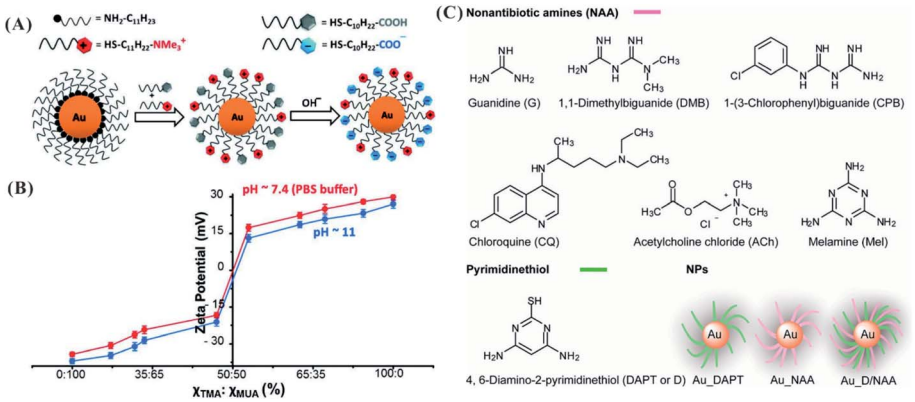

Fig. 7 The design of mixed-charge NPs. (A) The synthesis of mixed-charge NPs with different ratios of TMA/MUA. (B) The plotted curves of the NP charge polarities *vs.* the ratio of TMA : MUA. The blue and red curves are the zeta potentials at pH 11 and pH 7.4, respectively. The MUAs were fully deprotonated at pH 11, while a few MUAs were protonated at pH 7.4 (PBS buffer).[119] Reproduced from ref. 119 with permission from WILEY-VCH, Copyright© 2016. (C) The molecular structures of NAA and DAPT, and the synthesis of AuNPs using single or mixed ligands (including NAA and DAPT).[120] Reproduced from ref. 120 with permission from the American Chemical Society, Copyright© 2013.

Most ligands on NPs undergo nonspecific interactions with bacterial surfaces. The selectivity of nanomaterials on bacteria is of great significance to specifically kill pathogenic bacteria. In addition to charge-dependent Gram selectivity, some ligands binding specifically with bacteria have been used to coat NPs, such as antibodies, antibiotics, and trehalose. Antibodies conjugated to NPs allow the targeting of specific microbes. For example, AuNPs linked with antibodies can specifically induce the death of *Pseudomonas aeruginosa* under near-infrared irradiation.[122] Similarly, with the introduction of anti-protein A antibodies, AuNPs can selectively kill *S. aureus* under strong laser-induced overheating effects.[123] A similar specific antibacterial reaction against *S. aureus* appeared in lysostaphin-antibody-conjugated NPs.[124] In addition, vancomycin-conjugated AuNPs could specifically inhibit vancomycin-resistant and sensitive *Enterococci*.[125] The conjugation of trehalose can lead silica NPs to selectively bind with *Mycolicibacterium smegmatis* on *M. smegmatis*-treated A549 cells, contributing to the development of targeted therapy for the corresponding infectious disease.[126]

The charge-dependent antibacterial activity of some nanomaterials is shown in Table 2. The MIC of nanomaterials with cationic charges from different ligands were obtained from 1 μg mL^{-1} to 1 mg mL^{-1}, or from 16 nM to 112 μM.

3.4. Surface topography

In nature, the introduction of topological features endows natural substances with elevated surface adhesion ability. In the pollination of pollen grains by insects and the infection of host cells by viruses, the pollen and cells provide rough surfaces for multivalent interactions. Similar to the interaction of pollen and the hairy legs of honey bees in nature,[128] a hairy bacterial surface with pili[129] can bind robustly with pollen-like nanomaterials. The surface roughness of nanomaterials is of great significance to regulate the interactions between the nanomaterials and bacteria.[130] For example, designed nanoscale roughness on the surface of NPs is able to enhance attachment of bacteria to the nanomaterials.[131,132] By surface topographical modification, compared to smooth mesoporous hollow silica (MHS) with hydrophilic hydroxyl groups, MHS NPs with surface roughness obtained by adding silica shell particles became more hydrophobic due to the repulsion of trapped air in the

Table 2 The charge-dependent antibacterial activity of nanomaterials

No.	Nanomaterial	Ligand	Charge	Bacteria	MIC	Reference
1	AuNPs	Poly(allylamine hydrochloride)	Cationic	*Bacillus*	5 μg mL^{-1}	99
2	QD	Polyethylenimine	Cationic	*P. stutzeri*	IC_{50} at 7.25 ± 0.43 nM	100
3	Magnetic NPs	Quaternized poly(2-(dimethylamino)ethyl methacrylate)	Cationic	*E. coli*	1 mg mL^{-1}	106
4	Hydrogel	DMDC-Q-*g*-EM and poly(ethylene glycol)diacrylate	Cationic	*S. aureus*	49 μg mL^{-1}	109
5	AuNPs	Polythiophene	—	*Listeria monocytogenes*	112 μM	115
6	AuNPs	Pentanethiol	Cationic and hydrophobic group	*E. coli*	16 nM	127
7	AuNPs	1,1-Dimethylbiguanide and DAPT	Cationic	*E. coli*	1 μg mL^{-1}	120

void and cavity domains. The rough MHS NPs facilitate not only the controllable load and release of antibiotic vancomycin but also the enhanced interaction with bacteria.[133,134] Using three reagents, resorcinol (R), formaldehyde (F), and tetraethyl orthosilicate (TEOS), as the reactants through the Stöber method, the RF core was formed and subsequently underwent co-condensation with silica, producing rough mesoporous silica hollow spheres (RMSHSs) (named silica nanopollens) (Fig. 8A). The silica nanopollens with a spiky surface possess enhanced adhesion toward bacteria surfaces compared to their counterparts with smooth surfaces. Their accessible inner cavity can sufficiently load lysozymes, obtaining good antimicrobial activity toward *E. coli* (Fig. 8B).[135] In the design of nanomaterials, nature-inspired concepts can be introduced to build a novel library of antibacterial nanomaterials.

The surface topography is capable of affecting the affinity communication of a cell and the contact surface. The number and type of the bound cells depend on the topography of the used contact surface.[136] Especially, the topography and nanoscale roughness of synthetic surfaces play an important role in bacterial responses. For example, when using polyurethane-coated glass plates, the number of adherent bacteria is related to the surface roughness. The influence of the surface nanoroughness on the adhesion of bacteria is relative to the fimbriae, flagella or polymeric substances excreted by the bacteria.[137] The bacteria more readily aggregate on randomly ordered surfaces.[138] Microorganisms with different sizes and shapes possess different retentions on titanium-coated silicon wafers with size-regulated pits.[139] In addition, the surface topography can trigger and guide specific biological events. After treating bacteria with nanoscale metal substrates with a surface topography, the stress-related pathways of *E. coli* were activated by the nanorough surface. Different from the successful formation of bacterial fimbria on a flat surface (Fig. 9A), the synthesis of bacterial FimE protein on the nanorough surface is beneficial to convert the operon of the fimbrial promoter to the "OFF" status, inhibiting the transcription of all the fimbrial subunits and degrading the fimbrial structure (Fig. 9B).[140] However, in the above finding, surface roughness does not directly influence the number of adherent *E. coli*. The selected marine bacteria produce stronger attachments to smooth glass surfaces, accompanied by the increase of secreted extracellular polymeric substances.[141] Topography is only one factor for explaining the strong adhesion of bacteria. In addition to the surface topography, the adhesion between bacteria and the contact surface depends on the physicochemical properties of the substrates as well as the selected bacterial species and growing environment.

3.5. Shape

The shape regulation of nanomaterials can control the antibacterial activity of the nanomaterials due to the effect of different contact killings. To investigate the correlation between shape and antimicrobial activity, using poly(*N*-vinyl-2-pyrrolidone) (PVP) as the stabilizer, nanosilvers with different shapes were designed, such as silver nanoplates (AgNPLs), silver nanorods (AgNRs) and AgNPs. The AgNPLs produced the best antibacterial activity against *S. aureus* and *E. coli* due to their best surface area for interacting with the bacterial surface.[142] Similarly, compared to spherical and rod-shaped NPs, truncated triangular AgNPLs with more facets caused more membrane damage of bacteria, demonstrating strong antibacterial action,[31] consistent with previous studies.[85,143] Based on computer simulations, the anisotropy and initial orientation of the NPs affect the interaction between the NPs and the lipid bilayer in the translocation processes.[144] Rod-like silica NPs

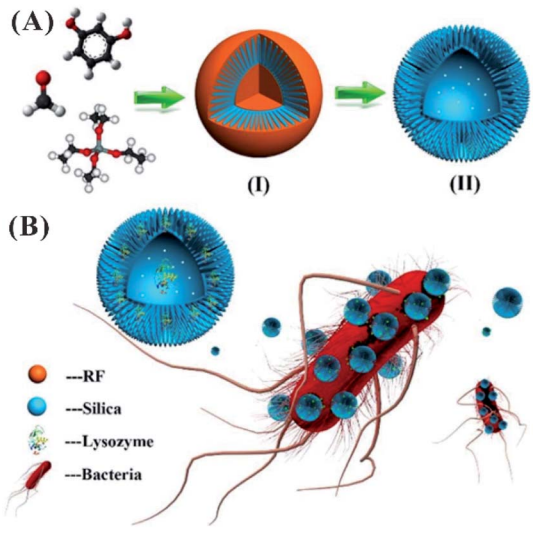

Fig. 8 Silica nanopollens for antibacterial effects. (A) The synthesis of silica nanopollens. (B) The delivery of lysozymes due to the enhanced adhesive reaction of silica nanopollens and the bacterial surface.[135] Reproduced from ref. 135 with permission from the American Chemical Society, Copyright© 2016.

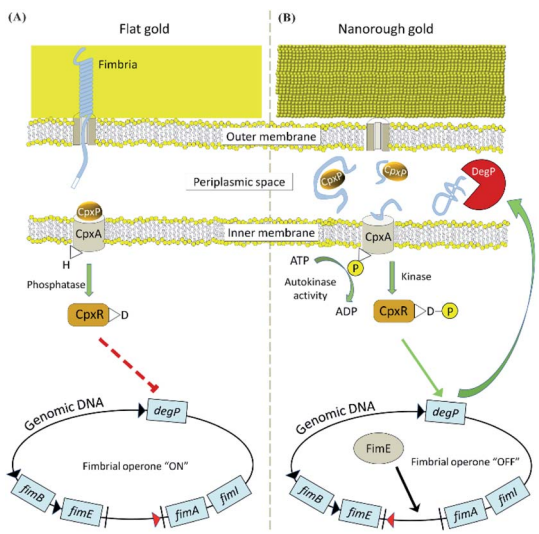

Fig. 9 The different molecular mechanisms of *E. coli* on flat (A) and nanorough (B) gold substrates.[140] The expression of type-1 fimbriae is active on the flat surface and inactive on the rough surface. Reproduced from ref. 140 with permission.

(AR8) for releasing nitric oxide produced greater antibacterial action than their spherical counterparts (AR1) due to their higher aspect ratio.[145]

A similar phenomenon occurs in the antibacterial operation of carbon nanomaterials.[40] Sharp edges of these graphene nanomaterials are important to the acquisition of excellent antibacterial activities. Graphene films with different edge lengths and different angles of orientation exhibit different antibacterial efficiencies against *P. aeruginosa* and *S. aureus*, which is attributed to the formation of pores in the bacterial cell wall.[146] In the graphene film, the presence of a smooth top side provides efficient inhibition for both types of bacteria, while the presence of a rough bottom side strongly kills only *P. aeruginosa*. Based on simulations, graphene sheets with corners or asperities along their irregular edges readily pierce and permeate into the cell membrane due to the existence of a low energy barrier.[147] GO nanowalls with sharp edges result in bacterial inactivation.[57] Needle-like single-walled carbon nanotubes and sharp-knife-like GO exhibit extremely strong antibacterial activity due to the destruction of the cell membrane.[148] Therefore, the antibacterial activity of nanomaterials can be regulated by rationally designing their shape.

3.6. The density of surface modification

The surfaces of Gram-positive and Gram-negative bacteria possess different charge distributions. Gram-negative bacteria have more negative surface charges than Gram-positive bacteria.[149] In addition to the limited selection of charge type, the charge density from surface ligands can regulate the antibacterial efficiency of nanomaterials. Using quaternized poly(-vinylpyridine) chains grafted on glass surfaces, the charge density of cationic ligands in the organic layer can be regulated within the range of 10^{12} and 10^{16} amines per cm^2.[150] The biocidal efficiency can be improved by increasing the charge density. The antibacterial activity is attributed to the removal of divalent counterions from the bacteria during the interactions between the bacteria and surfaces, inducing disruption of the bacterial envelope. By initially immobilizing cationic NPs or poly-L-lysine (PLL) and subsequently backfilling the remaining areas with PEG (polyethylene glycol) brushes, the obtained surface starts to perform obvious bacteria adhesion above the threshold of the modification density. Two distinct thresholds are needed using different surface modifications due to their different protrusions, such as ~180 NPs per μm^2 and ~1900 PLL per μm^2. Two kinds of test surfaces with low density (280 NPs per μm^2 and 3500 PLL per μm^2) were designed, establishing relatively weak bacterial adhesion.[151,152] The surfaces with NPs produced better killing efficiency of bacteria than those with PLL. Higher bactericidal efficiency was obtained on the surface with dense NPs.[153] However, a loose surface density is beneficial to remove the bacteria by moderate shearing flow (Fig. 10A).[154] The surface modification density using nanoparticles can regulate the adhesion and release of bacteria, affecting the antibacterial activity.

Based on the mixed self-assembled monolayers containing positively and negatively charged thiols, the cellular uptake of NPs with unique stability at low and high pH was regulated. The presence of positively charged thiols allows for the uptake of particles with net negative charges.[155] In addition to the tuned charge, the density of the ligands can regulate the antibacterial activity of NPs. By modification with different proportions of amine- and thiol-tethered phenylboronic acids *via* the binding affinities of Au–N and Au–S, including aminophenylboronic acid (ABA) and mercaptophenylboronic acid (MBA), the obtained AuNPs specifically bind to Gram-negative and Gram-positive bacteria. The AuNPs stabilized by ABA (A-AuNPs) bind to the lipopolysaccharide on Gram-negative bacteria, while the AuNPs stabilized by MBA (M-AuNPs) bind to the lipoteichoic acid on Gram-positive bacteria. The A-AuNPs and M-AuNPs show potent antibacterial effects on Gram-negative and Gram-positive bacteria, respectively. By co-modification of MBA and ABA on the AuNPs with varying ratios, the obtained A/M-AuNPs possess tunable antibacterial spectra with Gram selectivity (Fig. 10B).[156] The density of the selective ligand can contribute to regulation of the Gram-selective antibacterial activities of the nanomaterials.

3.7. Other factors

In addition to the above six main factors, other physicochemical properties of nanomaterials can affect their antibacterial activity performance, such as their stiffness and hydrophobicity. It is well known that graphene possesses high stiffness. With the introduction of oxygen functional groups, the mechanical properties of the produced well-dispersed GO are severely decreased.[157] GO with thin sheets may more readily wrap bacteria for performing antibacterial action.[40] Compared with their flexible counterparts, long and stiff CNTs have shown higher toxicity due to their compression arising from lysosomal membranes, leading to cell death.[158] The presence of polyacrylamide–gelatin–silver NPs or an *N*-acryloylsemicarbazide–gelatin scaffold can enhance the tensile and compression strength of gelatin-based ink, affording antibacterial properties.[159,160] However, research on the direct link between the antibacterial activity and stiffness of nanomaterials remains rare.

The hydrophobic interaction is a significant noncovalent reaction to control biomolecule absorption and cell adhesion in organisms.[161–163] Hydrophobic moieties (alkanethiols and alkyl chains) were used to form AuNPs[164,165] and silica NPs[166,167] for enhancing drug loading and cellular delivery. AuNPs were synthesized with ligands containing groups with different chain lengths, nonaromatic characteristics, and aromatic characteristics *via* the varied R groups (Fig. 11A). The hydrophobicity of the ligands on the surface of NPs can affect the antibacterial activity of NPs. AuNPs stabilized by ligands with higher hydrophobic values of their end groups led to more effective activity against *E. coli* growth. NP3 with *n*-decane end groups produced an MIC of 32 nM against *E. coli* (Fig. 11B).[127] The achievement of this antibacterial activity is attributed to the leakage of the cytoplasmic contents due to disruption of the bacterial membrane, eventually causing cell death. Even at 20 generations, *E. coli* remained susceptible to the original MIC of 16 nM.

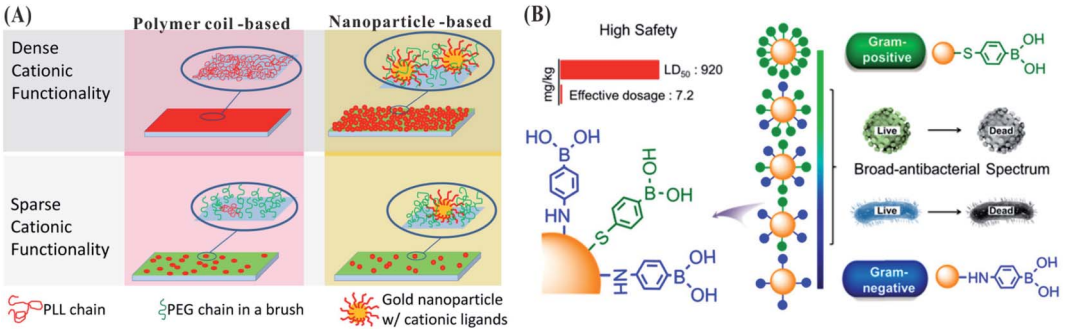

Fig. 10 (A) Design of surfaces with different modification densities and substrates. Red color indicates a ligand with a cationic charge, while green color indicates a neutral PEG brush.[154] Reproduced from ref. 154 with permission from the American Chemical Society, Copyright© 2014. (B) The design of AuNPs with different amounts and proportions of two ligands for obtaining bactericidal agents with tunable antibacterial spectra.[156] Reproduced from ref. 156 with permission from the American Chemical Society, Copyright© 2020.

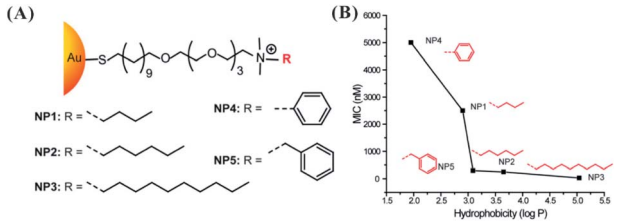

Fig. 11 (A) Molecular structures of functional ligands with different R groups for modifying AuNPs.[127] (B) MIC determination of AuNPs with different hydrophobic ligands against *E. coli* DH5R. Log *P* is the calculated hydrophobic values of the end groups.[127] Reproduced from ref. 127 with permission from the American Chemical Society, Copyright© 2014.

The design of NPs by regulating the types of modification groups can alleviate and avoid drug resistance. In addition, the increased hydrophobicity of AuNPs produced a linear increase in immune activity.[168] In the practical application of nanomaterials in the medical field, hydrophobicity-dependent immune effects should be fully considered.

4. Conclusions and outlook

The regulation of nanomaterials for obtaining customizable bactericidal agents is of great significance to inhibit the growth of pathogenic bacteria, providing more alternative strategies for treating infectious diseases. However, the reported literature has not systematically summarized the correlations between antibacterial activity and nanomaterials with various structures, leading to confusion of researchers regarding the rational design of antibacterial nanomaterials. To address these deficiencies, different from reported reviews that focus on the biological action of different antimicrobial NPs, this review summarized the universal rules determining the antibacterial activity of nanomaterials in six main aspects, including composition, size, charge, surface topography, shape and modification density. The clear description and discussion of every factor can provide precise guidance for constructing antibacterial nanomaterials.

The component selection of nanomaterials is the first factor for regulating their antibacterial activity. In addition to the innate antibacterial activity of AgNPs and CuNPs, NPs based on gold, zinc and titanium must be modified with ligands to exert their bactericidal effects by destroying cell integrity and forming ROS. Smaller size facilitates entry of nanomaterials into bacterial cells to perform their intracellular reactions, such as enzyme inactivation, DNA/RNA structure damage, and ROS formation. However, the action of the ligand should be considered in the size regulation. In the performance of antibacterial reactions, the binding of the nanomaterial and bacterial surface is the first step of the entry of the nanomaterial into bacterial cells. Due to the negatively charged properties of the bacterial surface, the introduction of cationic ligands is beneficial to enhance the antibacterial activity of nanomaterials. Interestingly, the introduction of neutral zwitterionic ligands can decrease the toxicity of nanomaterials with positive charge to mammalian cells. In addition, nanomaterials with a mixed ratio of cationic and anionic ligands can selectively and specifically kill Gram-positive or Gram-negative bacteria.

In addition to the charge effect, the surface topography of nanomaterials can regulate the adhesion of bacteria on the contact surface. Compared with a smooth surface, a rough surface is beneficial to enhance the interaction of bacteria and nanomaterials, leading to increased antibacterial activity. The selected bacterial species and growing environment may affect the adhesion of bacteria on the contact surface. The shape is another factor for regulating the antibacterial activity of nanomaterials. A shape with a high surface area is preferable to obtain good antibacterial activity. For example, silver nanoplates have higher antibacterial efficiency than silver nanorods and AgNPs. Rod-like NPs have higher activity than their spherical counterparts. The modification density of the surface of nanomaterials can regulate the interaction of nanomaterials and bacteria. The structure with dense modification is beneficial to bind with bacteria, producing excellent antibacterial activity. The density of the ligands can selectively inhibit Gram-positive and Gram-negative bacteria. In the real design of antibacterial nanomaterials, the involved factors should not be singly be considered due to the comprehensive antibacterial effect of nanomaterials.

Although antimicrobial nanomaterials are promising to become alternatives to antibiotics, their potential toxicity to human health remains uncertain. Due to nonspecific interactions with the bacterial surface, for most antimicrobial nanomaterials, it is difficult to specifically differentiate between microbial and human cells. More specific ligands for binding with bacteria should be found. The immune responses of nanomaterials as drugs should not be neglected. It is necessary to balance the death of bacteria and inflammatory reactions in the practical application of antimicrobial nanomaterials. Therefore, the direct replacement of common antibiotics with antimicrobial nanomaterials still has many large challenges. In the future, two significant tasks should receive more emphasis. Firstly, the effects of antimicrobial nanomaterials on health concerns and ecosystems should be investigated. Secondly, to promote the application of nanomaterials as antimicrobial agents, unified standards must be constructed to compare the antimicrobial effects of different nanomaterials.

In sum, this review provides alternative rules for designing a variety of antibacterial nanomaterials. By having a good understanding of the corresponding correlation between antibacterial activity and nanomaterials, researchers can follow the rules for precisely designing the properties of nanomaterials, finally achieving nanomaterials with maximized antibacterial activity in complex biological media and minimizing the cytotoxicity to host cells. The facile regulation of nanomaterials can provide alternative strategies for eradicating drug resistance and developing effective therapeutic next-generation materials. The achievement of effective antibacterial nanomaterials requires interdisciplinary collaborations of many researchers in the fields of chemistry, biology, medicine and engineering. The treatment strategies based on the regulated nanomaterials are promising to provide an alternative to antibiotics for intractable infections, alleviating the challenges of the post-antibiotic era.

Conflicts of interest

There are no conflicts to declare.

Acknowledgements

This work was financially supported by National Natural Science Foundation of China (NSFC Grants 21804089).

Notes and references

1 K. E. Jones, N. G. Patel, M. A. Levy, A. Storeygard, D. Balk, J. L. Gittleman and P. Daszak, *Nature*, 2008, **451**, 990–993.
2 A. P. Anisimov and K. K. Amoako, *J. Med. Microbiol.*, 2006, **55**, 1461–1475.
3 C. J. Leaver and J. Edelman, *Nature*, 1965, **207**, 1000–1001.
4 K. Kümmerer, *Chemosphere*, 2009, **75**, 417–434.
5 Q. Zhang, G. Lambert, D. Liao, H. Kim, K. Robin, C. K. Tung, N. Pourmand and R. H. Austin, *Science*, 2011, **333**, 1764–1767.
6 H. C. Neu, *Sci. Justice*, 1992, **257**, 1064–1073.
7 L. L. Ling, T. Schneider, A. J. Peoples, A. L. Spoering, I. Engels, B. P. Conlon, A. Mueller, T. F. Schäberle, D. E. Hughes, S. Epstein, M. Jones, L. Lazarides, V. A. Steadman, D. R. Cohen, C. R. Felix, K. A. Fetterman, W. P. Millett, A. G. Nitti, A. M. Zullo, C. Chen and K. Lewis, *Nature*, 2015, **517**, 455–459.
8 S. Reardon, *Nature*, 2015, **521**, 402–403.
9 K. M. G. O. Connell, J. T. Hodgkinson, H. F. Sore, M. Welch, G. P. C. Salmond and D. R. Spring, *Angew. Chem., Int. Ed.*, 2013, **52**, 10706–10733.
10 I. Yosef, M. Manor, R. Kiro and U. Qimron, *Proc. Natl. Acad. Sci. U. S. A.*, 2015, **112**, 7267–7272.
11 R. J. Citorik, M. Mimee and T. K. Lu, *Nat. Biotechnol.*, 2014, **32**, 1141–1145.
12 R. J. Krom, P. Bhargava, M. A. Lobritz and J. Collins, *Nano Lett.*, 2015, **15**, 4808–4813.
13 S. Galdiero, A. Falanga, R. Berisio, P. Grieco, G. Morelli and M. Galdiero, *Curr. Med. Chem.*, 2015, **22**, 1665–1677.
14 J. A. Lemire, J. J. Harrison and R. J. Turner, *Nat. Rev. Microbiol.*, 2013, **11**, 371–384.
15 K. P. Miller, L. Wang, B. C. Benicewicz and A. W. Decho, *Chem. Soc. Rev.*, 2015, **44**, 7787–7807.
16 S. Chernousova and M. Epple, *Angew. Chem., Int. Ed.*, 2013, **52**, 1636–1653.
17 K. Malzahn, W. D. Jamieson, M. Dröge, V. Mailänder, A. Jenkins, C. K. Weiss and K. Landfester, *J. Mater. Chem. B*, 2014, **2**, 2175–2183.
18 W. Zheng, Y. Jia, Y. Zhao, J. Zhang and X. Jiang, *Nano Lett.*, 2021, **21**, 1992–2000.
19 U. Bogdanovic, V. Lazic, V. Vodnik, M. Budimir, Z. Markovic and S. Dimitrijevic, *Mater. Lett.*, 2014, **128**, 75–78.
20 H. Yuan, Z. Liu, L. Liu, F. Lv, Y. Wang and S. Wang, *Adv. Mater.*, 2014, **26**, 4333–4338.
21 Y. Wang, H. Chen, M. Li, R. Hu, F. Lv, L. Liu and S. Wang, *Polym. Chem.*, 2016, **7**, 6699–6702.
22 H. Bai, H. Zhang, R. Hu, H. Chen, F. Lv, L. Liu and S. Wang, *Langmuir*, 2017, **33**, 1116–1120.
23 Q. Xin, H. Shah, A. Nawaz, W. Xie, M. Z. Akram, A. Batool, L. Tian, S. U. Jan, R. Boddula, B. Guo, Q. Liu and J. R. Gong, *Adv. Mater.*, 2019, **31**, 1804838.
24 L. Wang, H. Chen and L. Shao, *Int. J. Nanomed.*, 2017, **12**, 1227–1249.
25 M. E. Quadros and L. C. Marr, *Environ. Sci. Technol.*, 2011, **45**, 10713–10719.
26 J. S. Kim, E. Kuk, K. N. Yu, J. H. Kim, S. J. Park, J. L. Hu, S. H. Kim, Y. K. Park, H. P. Yong and C. Y. Hwang, *Nanomedicine*, 2007, **3**, 95–101.
27 L. Rizzello and P. P. Pompa, *Chem. Soc. Rev.*, 2014, **43**, 1501–1518.
28 Z. Xiu, Q. Zhang, H. L. Puppala, V. L. Colvin and P. J. J. Alvarez, *Nano Lett.*, 2012, **12**, 4271–4275.
29 O. Choi and Z. Hu, *Environ. Sci. Technol.*, 2008, **42**, 4583–4588.
30 A. E. Badawy, R. G. Silva, B. Morris, K. G. Scheckel, M. T. Suidan and T. M. Tolaymat, *Environ. Sci. Technol.*, 2010, **45**, 283–287.

31 S. Pal, K. T. Yu and J. M. Song, *Appl. Environ. Microbiol.*, 2007, **73**, 1712–1720.
32 Y. Inoue, M. Hoshino, H. Takahashi, T. Noguchi, T. Murata, Y. Kanzaki, H. Hamashima and M. Sasatsu, *J. Inorg. Biochem.*, 2002, **92**, 37–42.
33 R. Kumar and H. Münstedt, *Biomaterials*, 2005, **26**, 2081–2088.
34 M. Lv, S. Su, Y. He, Q. Huang, W. Hu, D. Li, C. Fan and S. T. Lee, *Adv. Mater.*, 2010, **22**, 5463–5467.
35 K. Zheng and J. Xie, *ACS Nano*, 2020, **14**, 11533–11541.
36 B. Hisey, P. J. Ragogna and E. R. Gillies, *Biomacromolecules*, 2017, **18**, 914–923.
37 T. Gao, H. Fan, X. Wang, Y. Gao and Y. J. Wang, *ACS Appl. Mater. Interfaces*, 2017, **9**, 25738–25746.
38 H. E. Karahan, C. Wiraja, C. Xu, J. Wei and C. Yuan, *Adv. Healthcare Mater.*, 2018, **7**, 1701406.
39 A. J. Ahmed, A. Surjith, B. Kateryna and J. Mohan, *Mater. Corros.*, 2017, **10**, 1066.
40 X. Zou, Z. Li, Z. Wang and Y. Luo, *J. Am. Chem. Soc.*, 2016, **138**, 2064–2077.
41 X. Chen and H. J. Schluesener, *Toxicol. Lett.*, 2008, **176**, 1–12.
42 Y. Zhao and X. Jiang, *Nanoscale*, 2013, **5**, 8340–8350.
43 M. J. Hajipour, K. M. Fromm, A. A. Ashkarran, D. D. Aberasturi, I. Larramendi, T. Rojo, V. Serpooshan, W. J. Parak and M. Mahmoudi, *Trends Biotechnol.*, 2012, **20**, 499–511.
44 A. Gupta, S. Mumtaz, C. H. Li, I. Hussain and V. M. Rotello, *Chem. Soc. Rev.*, 2019, **48**, 415–427.
45 A. F. Halbus, T. S. Horozov and V. N. Paunov, *Adv. Colloid Interface Sci.*, 2017, **249**, 134–148.
46 A. P. Ingle, N. Duran and M. Rai, *Appl. Microbiol. Biotechnol.*, 2014, **98**, 1001–1009.
47 J. Makabenta, A. Nabawy, C. H. Li, S. Schmidt-Malan and V. M. Rotello, *Nat. Rev. Microbiol.*, 2021, **19**, 23–36.
48 A. Gupta, R. F. Landis and V. M. Rotello, *F1000Research*, 2016, **5**, 364.
49 S. Shahzadi, Z. Noshin, R. Saira, S. Rehana, N. Jawad and N. Shahzad, *Nanomaterials*, 2016, **6**, 1–10.
50 A. K. Chatterjee, R. Chakraborty and T. BaSu, *Nanotechnology*, 2014, **25**, 135101.
51 Y. Zhao, Y. Tian, C. Yan, W. Liu, W. Ma and X. Jiang, *J. Am. Chem. Soc.*, 2010, **132**, 12349–12356.
52 M. Vincent, R. E. Duval, P. Hartemann and M. Engels-Deutsch, *J. Appl. Microbiol.*, 2017, **124**, 1032–1046.
53 G. Grass, C. Rensing and M. Solioz, *Appl. Environ. Microbiol.*, 2011, **77**, 1541–1547.
54 Y. Liu, N. Nie, H. Tang, C. Zhang, K. Chen, W. Wang and J. Liu, *ACS Appl. Mater. Interfaces*, 2021, **13**, 11631–11645.
55 B. Hammer and J. K. Norskov, *Nature*, 1995, **376**, 238–240.
56 A. Sirelkhatim, S. Mahmud, A. Seeni, N. Kaus, C. A. Ling, S. Bakhori, H. Hasan and D. Mohamad, *Nano-Micro Lett.*, 2015, **7**, 219–242.
57 O. Akhavan and E. Ghaderi, *ACS Nano*, 2010, **4**, 5731–5736.
58 Y. Tu, M. Lv, P. Xiu, T. Huynh, M. Zhang, M. Castelli, Z. Liu, Q. Huang, C. Fan and H. Fang, *Nat. Nanotechnol.*, 2013, **8**, 594–601.
59 M. Lee, S. Yang, K. J. Kim, S. Kim and H. Lee, *J. Phys. Chem. C*, 2014, **118**, 1142–1147.
60 S. Kang, M. Herzberg, D. F. Rodrigues and M. Elimelech, *Langmuir*, 2008, **24**, 6409–6413.
61 S. Liu, L. Wei, L. Hao, N. Fang and Y. Chen, *ACS Nano*, 2009, **3**, 3891–3902.
62 S. Kang, M. Pinault, L. D. Pfefferle and M. Elimelech, *Langmuir*, 2007, **23**, 8670–8673.
63 M. C. Daniel and D. Astruc, *Chem. Rev.*, 2004, **104**, 293–346.
64 A. M. Alkilany, X. Huang, C. J. Murphy, M. A. El-Sayed and E. C. Dreaden, *Chem. Soc. Rev.*, 2012, **41**, 2740.
65 J. Kneipp, H. Kneippa and K. Kneippa, *Chem. Soc. Rev.*, 2008, **37**, 1052–1060.
66 X. Zhou, W. Xu, G. Liu, D. Panda and P. Chen, *J. Am. Chem. Soc.*, 2010, **132**, 138–146.
67 D. Alloyeau, C. Ricolleau, C. Mottet, T. Oikawa, C. Langlois, Y. L. Bouar, N. Braidy and A. Loiseau, *Nat. Mater.*, 2009, **8**, 940–946.
68 B. L. Li, M. I. Setyawati, H. L. Zou, J. X. Dong, H. Q. Luo, N. B. Li and D. T. Leong, *Small*, 2017, **13**, 1700527.
69 A. Albanese, P. S. Tang and W. Chan, *Annu. Rev. Biomed. Eng.*, 2012, **14**, 1–16.
70 W. Jiang, B. Kim, J. T. Rutka and W. Chan, *Nat. Nanotechnol.*, 2008, **3**, 145–150.
71 C. He, Y. Hu, L. Yin, C. Tang and C. Yin, *Biomaterials*, 2010, **31**, 3657–3666.
72 P. Yu, S. Neuss, A. Leifert, M. Fischler and W. Jahnen-Dechent, *Small*, 2007, **3**, 1941–1949.
73 M. I. Setyawati, C. Y. Tay, B. H. Bay and D. T. Leong, *ACS Nano*, 2017, **11**, 5020–5030.
74 M. I. Setyawati and D. T. Leong, *ACS Appl. Mater. Interfaces*, 2017, **9**, 6690–6703.
75 K. Zheng, M. I. Setyawati, T. P. Lim, D. T. Leong and J. Xie, *ACS Nano*, 2016, **10**, 7934–7942.
76 X. Yuan, M. I. Setyawati, A. S. Tan, C. N. Ong, D. T. Leong and J. Xie, *NPG Asia Mater.*, 2013, **5**, e39.
77 K. Zheng, M. I. Setyawati, D. T. L. Orcid and J. Xie, *ACS Nano*, 2017, **11**, 6904–6910.
78 O. Yamamoto, *Int. J. Inorg. Mater.*, 2001, **3**, 643–646.
79 K. R. Raghupathi, R. T. Koodali and A. C. Manna, *Langmuir*, 2011, **27**, 4020–4028.
80 M. Yamanaka, K. Hara and J. Kudo, *Appl. Environ. Microbiol.*, 2005, **71**, 7589–7593.
81 C. Carlson, S. M. Hussain, A. M. Schrand, L. K. Braydich-Stolle, K. L. Hess, R. L. Jones and J. J. Schlager, *J. Phys. Chem. B*, 2008, **112**, 13608–13619.
82 G. A. Martínez-Castaón, N. Nio-Martínez, F. Martínez-Gutierrez, J. Martínez-Mendoza and F. Ruiz, *J. Nanopart. Res.*, 2008, **10**, 1343–1348.
83 A. Ivask, O. Bondarenko, N. Jepihhina and A. Kahru, *Anal. Bioanal. Chem.*, 2010, **398**, 701–716.
84 Q. L. Feng, J. Wu, G. Q. Chen, F. Z. Cui and J. O. Kim, *J. Biomed. Mater. Res.*, 2000, **52**, 662–668.
85 J. R. Morones, J. L. Elechiguerra, A. Camacho, K. Holt, J. B. Kouri, J. Ramírez and M. J. Yacaman, *Nanotechnology*, 2005, **16**, 2346–2353.

86 S. Huo, Y. Jiang, A. Gupta, Z. Jiang, R. F. Landis, S. Hou, X. Liang and V. M. Rotello, *ACS Nano*, 2016, **10**, 8732–8737.
87 S. C. Hayden, G. Zhao, K. Saha, R. L. Phillips, X. Li, O. R. Miranda, V. M. Rotello, M. A. El-Sayed, I. Schmidt-Krey and U. H. F. Bunz, *J. Am. Chem. Soc.*, 2012, **134**, 6920–6923.
88 M. J. Hostetler, A. C. Templeton and R. W. Murray, *Langmuir*, 1999, **15**, 3782–3789.
89 M. Brust, M. Walker, D. Bethell, D. J. Schiffrin and R. Whyman, *Chem. Commun.*, 1994, 801–802.
90 A. Panáček, L. Kvítek, M. Smékalová, R. Večeřová, M. Kolář, M. Röderová, F. Dyčka, M. Šebela, R. Prucek, O. Tomanec and R. Zbořil, *Nat. Nanotechnol.*, 2018, **13**, 65–71.
91 W. Zheng, Y. Jia, W. Chen, G. Wang, X. Guo and X. Jiang, *ACS Appl. Mater. Interfaces*, 2017, **9**, 21181–21189.
92 C. Yan, Y. Zhao, Y. Tian, Z. Wei, X. Lü and X. Jiang, *Biomaterials*, 2012, **33**, 2327–2333.
93 A. M. Carmona-Ribeiro and L. D. de Melo Carrasco, *Int. J. Mol. Sci.*, 2013, **14**, 9906–9946.
94 R. Hancock and H. G. Sahl, *Nat. Biotechnol.*, 2006, **24**, 1551–1557.
95 K. A. Brogden, *Nat. Rev. Microbiol.*, 2005, **3**, 238–250.
96 V. Sambhy, B. R. Peterson and A. Sen, *Angew. Chem., Int. Ed.*, 2008, **47**, 1250–1254.
97 L. Liu, K. Xu, H. Wang, P. J. Tan, W. Fan, S. S. Venkatraman, L. Li and Y. Y. Yang, *Nat. Nanotechnol.*, 2009, **4**, 457–463.
98 F. Nederberg, Y. Zhang, J. Tan, K. Xu, H. Wang, C. Yang, S. Gao, X. D. Guo, K. Fukushima and L. Li, *Nat. Chem.*, 2011, **3**, 409–414.
99 Z. V. Feng, L. L. Gunsolus, T. A. Qiu, K. R. Hurley, L. H. Nyberg, H. Frew, K. P. Johnson, A. M. Vartanian, L. M. Jacob, S. E. Lohse, M. D. Torelli, R. J. Hamers, C. J. Murphyc and C. L. Haynes, *Chem. Sci.*, 2015, **6**, 5186–5196.
100 Y. Yu, H. Zhu, V. L. Colvin and P. J. Alvarez, *Environ. Sci. Technol.*, 2011, **45**, 4988–4994.
101 J. Wang, Y. P. Chen, K. Yao, P. A. Wilbon, W. Zhang, L. Ren, J. Zhou, M. Nagarkatti, C. Wang and F. Chu, *Chem. Commun.*, 2011, **48**, 916–918.
102 S. Imazato, M. Torii, Y. Tsuchitani, J. F. Mccabe and R. Russell, *J. Dent. Res.*, 1994, **73**, 1437–1443.
103 S. Chemburu, T. S. Corbitt, L. K. Ista, E. Ji, J. Fulghum, G. P. Lopez, K. Ogawa, K. S. Schanze and D. G. Whitten, *Langmuir*, 2008, **24**, 11053–11062.
104 L. Lu, F. H. Rininsland, S. K. Wittenburg, K. E. Achyuthan, D. W. Mcbranch and D. G. Whitten, *Langmuir*, 2005, **21**, 10154–10159.
105 T. S. Corbitt, J. R. Sommer, S. Chemburu, K. Ogawa, L. K. Ista, G. P. Lopez, D. G. Whitten and K. S. Schanze, *ACS Appl. Mater. Interfaces*, 2009, **1**, 48–52.
106 H. Dong, J. Huang, R. R. Koepsel, P. Ye, A. J. Russell and K. Matyjaszewski, *Biomacromolecules*, 2011, **12**, 1305–1311.
107 C. E. Codling, M. Jean-Yves and R. A. Denver, *J. Antimicrob. Chemother.*, 2003, 1153–1158.
108 V. Berry, A. Gole, S. Kundu, C. J. Murphy and R. F. Saraf, *J. Am. Chem. Soc.*, 2005, **127**, 17600–17601.
109 P. Li, Y. F. Poon, W. Li, H. Y. Zhu, S. H. Yeap, Y. Cao, X. Qi, C. Zhou, M. Lamrani and R. W. Beuerman, *Nat. Mater.*, 2011, **10**, 149–156.
110 C. M. oodman, C. D. McCusker, T. Yilmaz and V. M. Rotello, *Bioconjugate Chem.*, 2004, **15**, 897–900.
111 Z. Zhang, Z. Min, S. Chen, T. A. Horbett, B. D. Ratner and S. Jiang, *Biomaterials*, 2008, **29**, 4285–4291.
112 S. Jiang and Z. Cao, *Adv. Mater.*, 2010, **22**, 920–932.
113 G. Cheng, Z. Zhang, S. Chen, J. D. Bryers and S. Jiang, *Biomater., Artif. Cells, Artif. Organs*, 2007, **28**, 4192–4199.
114 J. Bresee, K. E. Maier, A. E. Boncella, C. Melander and D. L. Feldheim, *Small*, 2011, **7**, 2027–2031.
115 M. Adhikari, S. Goswami, B. R. Panda, A. Chattopadhyay and A. Ramesh, *Adv. Healthcare Mater.*, 2013, **2**, 599–606.
116 X. Zheng, Y. Su, Y. Chen, R. Wan, M. Li, Y. Wei and H. Huang, *Sci. Rep.*, 2014, **4**, 5653.
117 R. Crh and C. Whitfield, *Annu. Rev. Biochem.*, 2002, **71**, 635–700.
118 J. van Heijenoort, *Glycobiology*, 2001, **11**, 25R–36R.
119 P. P. Pillai, B. Kowalczyk, K. Kandere-Grzybowska, M. Borkowska and B. A. Grzybowski, *Angew. Chem., Int. Ed.*, 2016, **55**, 8610–8614.
120 Y. Zhao, Z. Chen, Y. Chen, J. Xu, J. Li and X. Jiang, *J. Am. Chem. Soc.*, 2013, **135**, 12940–12943.
121 A. M. Fayaz, K. Balaji, M. Girilal, R. Yadav, P. T. Kalaichelvan and R. Venketesan, *Nanomedicine*, 2010, **6**, 103–109.
122 R. S. Norman, J. W. Stone, A. Gole, C. J. Murphy and T. L. Sabo-Attwood, *Nano Lett.*, 2008, **8**, 302–306.
123 V. P. Zharov, K. E. Mercer, E. N. Galitovskaya and M. S. Smeltzer, *Biophys. J.*, 2006, **90**, 619–627.
124 R. Satishkumar and A. A. Vertegel, *Nanotechnology*, 2011, **22**, 505103.
125 H. Gu, P. L. Ho, E. Tong, L. Wang and B. Xu, *Nano Lett.*, 2003, **3**, 1261–1263.
126 K. W. Jayawardana, H. S. N. Jayawardena, S. A. Wijesundera, T. D. Zoysa, M. Sundhoroa and M. Yan, *Chem. Commun.*, 2015, **51**, 12028–12031.
127 X. Li, S. M. Robinson, A. Gupta, K. Saha and V. M. Rotello, *ACS Nano*, 2014, **8**, 10682–10686.
128 R. W. Thorp, *Plant Syst. Evol.*, 2000, **222**, 211–223.
129 L. Craig, M. E. Pique and J. A. Tainer, *Nat. Rev. Microbiol.*, 2004, **2**, 363–378.
130 C. Meng, Q. Yu and H. Sun, *Int. J. Mol. Sci.*, 2013, **14**, 18488–18501.
131 E. P. Ivanova, V. K. Truong, J. Y. Wang, C. C. Berndt, R. T. Jones, I. I. Yusuf, I. Peake, H. W. Schmidt, C. Fluke, D. Barnes and R. J. Crawford, *Langmuir*, 2010, **26**, 1973–1982.
132 V. K. Truong, R. Lapovok, Y. S. Estrin, S. Rundell, J. Y. Wang, C. J. Fluke, R. J. Crawford and E. P. Ivanova, *Biomaterials*, 2010, **31**, 3674–3683.
133 Y. A. Nor, Y. Niu, S. Karmakar, L. Zhou, C. Xu, J. Zhang, H. Zhang, M. Yu, D. Mahony, N. Mitter, M. A. Cooper and C. Yu, *ACS Cent. Sci.*, 2015, **1**, 328–334.
134 X. Wu, Y. Tian, Y. Cui, L. Wei, Q. Wang and Y. Chen, *J. Phys. Chem. C*, 2007, **27**, 9704–9708.

135 S. Hao, Y. A. Nor, M. Yu, Y. Yang and C. Yu, *J. Am. Chem. Soc.*, 2016, **138**, 6455–6462.
136 E. Yim and K. W. Leong, *Nanomedicine*, 2005, **1**, 10–21.
137 D. P. Bakker, H. J. Busscher, J. v. Zanten, J. d. Vries, J. W. Klijnstra and H. C. v. d. Mei, *Microbiology*, 2004, **150**, 1779–1784.
138 C. Díaz, P. L. Schilardi, R. C. Salvarezza and M. F. de Mele, *Langmuir*, 2007, **23**, 11206–11210.
139 K. A. Whitehead, J. Colligon and J. Verran, *Colloids Surf., B*, 2005, **41**, 129–138.
140 L. Rizzello, A. Galeone, G. Vecchio, V. Brunetti, S. Sabella and P. P. Pompa, *Nanoscale Res. Lett.*, 2012, **7**, 575.
141 N. Mitik-Dineva, J. Wang, V. K. Truong, P. R. Stoddart, F. Malherbe, R. J. Crawford and E. P. Ivanova, *Biofouling*, 2009, **25**, 621–631.
142 B. Sadeghi, F. S. Garmaroudi, M. Hashemi, H. R. Nezhad, A. Nasrollahi, S. Ardalan and S. Ardalan, *Adv. Powder Technol.*, 2012, **23**, 22–26.
143 I. Sondi and B. Salopek-Sondi, *J. Colloid Interface Sci.*, 2004, **275**, 117–182.
144 K. Yang and Y. Q. Ma, *Nat. Nanotechnol.*, 2010, **5**, 579–583.
145 D. L. Slomberg, Y. Lu, A. D. Broadnax, R. A. Hunter and M. H. Schoenfisch, *ACS Appl. Mater. Interfaces*, 2013, **5**, 9322–9329.
146 V. Pham, V. K. Truong, M. Quinn, S. M. Notley, Y. Guo, V. A. Baulin, M. A. Kobaisi, R. J. Crawford and E. P. Ivanova, *ACS Nano*, 2015, **9**, 8458–8467.
147 Y. Li, H. Yuan, D. Von, M. Creighton, R. H. Hurt, A. B. Kane and H. Gao, *Proc. Natl. Acad. Sci. U. S. A.*, 2013, **110**, 12295–12300.
148 X. Wang, X. Liu and H. Han, *Colloids Surf., B*, 2013, **103**, 136–142.
149 Y. Shai, *Biopolymers*, 2002, **66**, 236–248.
150 R. Kügler, O. Bouloussa and F. Rondelez, *Microbiology*, 2005, **151**, 1341–1348.
151 B. Fang, S. Gon, M. Park, K. N. Kumar, V. M. Rotello, K. Nusslein and M. M. Santore, *Colloids Surf., B*, 2011, **87**, 109–115.
152 S. Gon, K. N. Kumar, K. Nüsslein and M. M. Santore, *Macromolecules*, 2012, **45**, 8373–8381.
153 B. Fang, Y. Jiang, K. Nüsslein, V. M. Rotello and M. M. Santore, *Colloids Surf., B*, 2015, **125**, 255–263.
154 B. Fang, Y. Jiang, V. M. Rotello, K. Nüsslein and M. M. Santore, *ACS Nano*, 2014, **8**, 1180–1190.
155 P. P. Pillai, S. Huda, B. Kowalczyk and B. A. Grzybowski, *J. Am. Chem. Soc.*, 2013, **135**, 6392–6395.
156 L. Wang, S. Li, J. Yin, J. Yang, Q. Li, W. Zheng, S. Liu and X. Jiang, *Nano Lett.*, 2020, **20**, 5036–5042.
157 A. J. Clancy, D. B. Anthony and F. D. Luca, *ACS Appl. Mater. Interfaces*, 2020, **12**, 15955–15975.
158 W. Zhu, V. Annette, X. Yi, Y. Qiu, Z. Wang, P. Weston, R. H. Hurt, A. B. Kane and H. Gao, *Proc. Natl. Acad. Sci. U. S. A.*, 2016, **113**, 12374–12379.
159 Y. Liu, J. Huang, Z. Xu, S. Li, Y. Jiang, G. w. Qu, Z. Li, Y. Zhao, X. Wu and J. Ren, *Int. J. Biol. Macromol.*, 2021, **186**, 396–404.
160 R. Yang, C. Fan, Y. Dou, X. Zhang, Z. Xu, Q. Zhang, Y. Sun, Q. Yang and W. Liu, *Appl. Mater. Today*, 2021, **24**, 101089.
161 T. Cedervall, I. Lynch, S. Lindman, T. Berggard, E. Thulin, H. Nilsson, K. A. Dawson and S. Linse, *Proc. Natl. Acad. Sci. U. S. A.*, 2007, **104**, 2050–2055.
162 A. E. Nel, L. Mädler, D. Velegol, T. Xia, E. M. V. Hoek, P. Somasundaran, F. Klaessig, V. Castranova and M. Thompson, *Nat. Mater.*, 2009, **8**, 543–557.
163 M. B. Salerno, B. E. Logan and D. Velegol, *Langmuir*, 2004, **20**, 10625–10629.
164 A. Sethuraman, M. Han, R. S. Kane and G. Belfort, *Langmuir*, 2004, **20**, 7779–7788.
165 M. R. Rasch, E. Rossinyol, J. L. Hueso, B. W. Goodfellow, J. Arbiol and B. A. Korgel, *Nano Lett.*, 2010, **10**, 3733–3739.
166 S. S. Bale, S. J. Kwon, D. A. Shah, A. Banerjee and R. S. Kane, *ACS Nano*, 2010, **4**, 1493–1500.
167 J. Zhang, S. Karmakar, M. Yu, N. Mitter, J. Zou and C. Yu, *Small*, 2015, **10**, 5068–5076.
168 D. F. Moyano, M. Goldsmith, D. J. Solfiell, D. Landesman-Milo, O. R. Miranda, P. Dan and V. M. Rotello, *J. Am. Chem. Soc.*, 2012, **134**, 3965–3967.